A Method of Data Reduction to Obtain the Two-Dimensional Aerodynamic Characteristics of a Circular Cylinder with Tangential Blowing

by

Ryoji WAKA* and Fumio YOSHINO*

(Received June 11, 1982)

Three different methods of data reduction were devised to determine the induced angle of attack of a circular cylinder with tangential blowing as a function of lift coefficient. The experimental values were corrected by making use of the induced angle of attack thus obtained. Consequently, the most recommended method of them was chosen to obtain the two-dimensional aerodynamic characteristics of the cylinder, and some examples of them were presented.

1 Introduction

In general the experiments on two-dimensional aerodynamic characteristics of various bodies such as an airfoil, a circular cylinder and so forth have been carried out at the mid-span of a two-dimensional model by taking the symmetry into account. Then the so-called two-dimensional model is the one which has usually end-plates at both ends of the model or spans both side-walls of the test section so as to keep two-dimensionality of the main flow. However, the author's found from the investigation[1] on a circular cylinder with tangential blowing that even if the model was the two-dimensional one, the flow near the cylinder-side-wall juncture was a complex three-dimensional flow composed of three kinds of vortices which rolled up a strong trailing vortex downstream of the cylinder.

Therefore the experimental values on aerodynamic characteristics obtained at the mid-span of a two-dimensional model are influenced by the induced angle of attack. Though it is necessary to eliminate this effect from the experimental values for determination of the two-dimensional characteristics of the cylinder, the estimation of this induced angle of attack is very difficult under present condition, because of the lack of the known "true" two-dimensional characteristic values and also the breakdown of the Kutta-Joukowsky condition in this case.

In this report three different simpler methods of data reduction are described to determine the induced angle of attack at the mid-span as a function of lift coefficient. Some examples corrected by the most recommended method of them are presented for a circular cylinder with tangential blowing.

* Department of Mechanical Engineering.

2 Nomenclature

C_l, $C_l(O)$: sectional lift coefficient at the mid-span
C_d, $C_d(O)$: sectional drag coefficient at the mid-span
C_p : pressure coefficient
C_μ : (momentum of the jet per unit span)/ $\{(1/2)\rho U^2 D\}$
D : diameter of the model cylinder
Re : Reynolds number $(=UD/\nu)$
U : velocity of the uniform flow
y : coordinate taken in the starboard direction from the mid-span
θ_j : angular location of the blowing slot
θ_m : angular location of the minimum pressure point
θ_{sb} : angular width of the separation region
θ_u : angular location of the upper separation point
α_i : induced angle of attack
λ : aspect ratio of the model cylinder
ν : kinematic viscosity coefficient
suffix ∞ indicates the two-dimensional value.

3 Experimental apparatus and method

The apparatus for this experiment was the same one as described in the references (2) and (3), and it is not described here in detail.

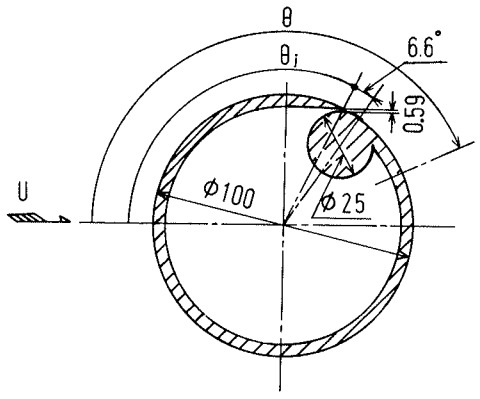

Fig. 1 Cross section of the model cylinder.

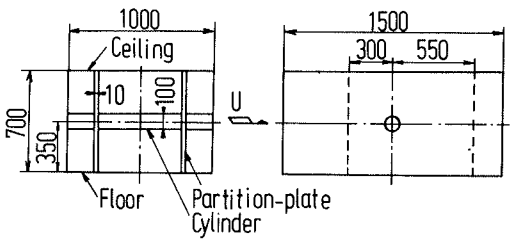

Fig. 2 Test section of the wind tunnel.

Figs. 1 and 2 show the cross section of the model cylinder and the test section of the wind tunnel, respectively. The diameter of the cylinder, D, is $100mm$ and the height of the blowing slot is constant, $0.59mm$, across the whole span. The static-pressure holes of 335 in number in all are distributed circumferencially at ten spanwise locations on the cylinder. The model

cylinder is mounted at the center of the test section and passes through two partition-plates (hereinafter referred to as "side-wall"). The structure of the cylinder-side-wall juncture is the same one that is shown in Fig. 4(a) of the reference (3) or Fig.1(b) of the reference (4).

The experiment was carried out by varing λ, θ_j and $C\mu$ under the condition of constant Re of 2.1×10^5. When $\lambda=4$ and 6, θ_j was kept constant at 90°. On the other hand, when $\lambda=8$, three different locations of θ_j were used, that is, $\theta_j=50°$, 90° and 120°. $C\mu$ was varied from 0 to about 0.3 for all the cases mentioned above.

The spanwise and circumferential static-pressure distibutions were measured with a multitube manometer.

4 Experimental result

Fig. 3 shows the relation between θ_m and C_l (θ_m-C_l relation). θ_m increases gradually with the increase of C_l. It is found from this figure that the minimum pressure point on the cylinder, except the one due to jet, moves downstream and the influence of λ on θ_m begins to appear, as C_l increases.

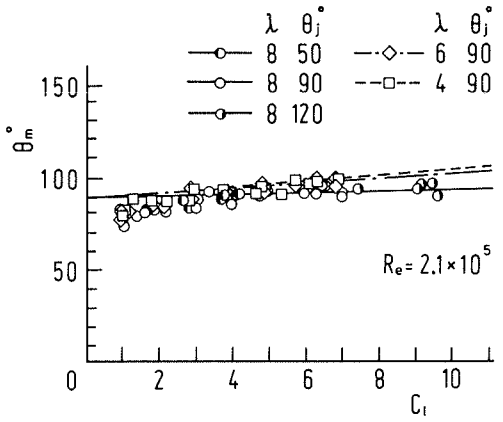

Fig. 3 Relation between θ_m and C_l.

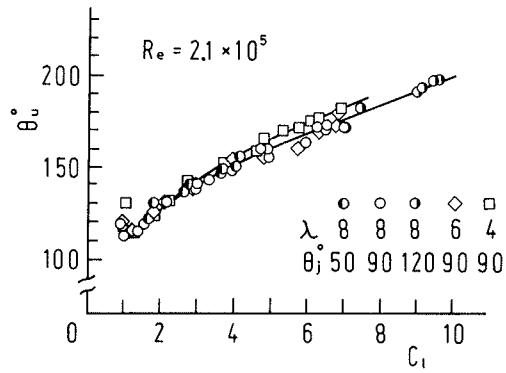

Fig. 4 Relation between θ_u and C_l.

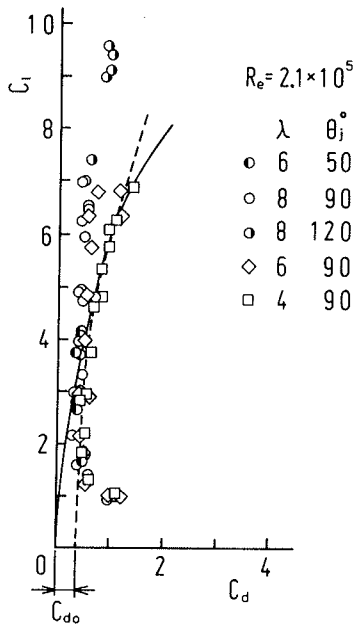

Fig. 5 Relation between C_l and C_d.

Fig. 4 shows θ_u-C_l relation. θ_u increases monotonically with the increase of C_l except when C_l is considerably small. The influence of λ on θ_u appears between $\lambda=4$ and $\lambda=6$, 8, as C_l increases.

Fig. 5 shows C_l-C_d relation. When C_l increases, C_d decreases once and takes the minimum value, after that C_d increases again as C_l increases. C_d is mainly given by the sum of the profile drag coefficient, C_{do}, and the induced drag coefficient, C_{di}, in this experimental Reynolds number. And C_{do} decreases to nearly zero almost independently of λ and C_{di} increases depending on λ as C_l increases. Taking account of this, the behavior of C_d against C_l mentioned above can be explained by considering the ratio of the increment of C_{di} to that of C_l when C_l is large. When C_l is large, dC_{di}/dC_l and the value of C_d for each of $\lambda=4$, 6 and 8 become smaller as λ increases. Then the influence of λ on C_d appears as C_l increases.

5 Discussion

5-1 The method of determination of the induced angle of attack

Two effects must be considered to obtain the two-dimensional characteristics from the experimental values of the cylinder with tangential blowing. One of them is the effect of the side-wall and the other is that of the induced angle of attack. The range affected by the side-wall has been already evidenced experimentally for this model cylinder, and it was $1.8D$, at the maximum, from the side-wall toward the mid-span[2]. Then if $\lambda \geqq 4$, the two-dimensional characteristic values are obtained from the experimental ones at the mid-span by correcting the effect of the induced angle of attack.

In this report three different simpler methods are devised to determine α_i by considering the following two experimental facts. First, when C_l is large enough, the flow around the cylinder is approximately a potential flow with circulation around it. Second, the spanwise distributions of C_{ln}, lift coefficient normalized by C_l, are congruent and independent of C_μ, and they are almost exclusively dependent on λ only (not shown here).

Now each method is described below.

(1) The method of theoretical calculation (method (1))

This method has been already described in detail in our reports[2],[3]. Now we give only an outline of this method. In this method some assumptions were made to calculate α_i. Taking the interference of the side-walls into account, the lifting line theory was applied to estimate α_i due to the trailing-shed vortex only, neglecting that due to the trailing-filament vortex.

Then the spanwise distribution of α_i along the cylinder axis is given as follows,

$$\alpha_i = -\frac{\pi}{4}\sum_{n=1}^{\infty} n a_n \cos\frac{n\pi}{B} y \tanh\frac{n\pi}{B} H, \qquad \cdots\cdots(1)$$

where B is the semi-span of the cylinder, $-B \leqq y \leqq B$, and H is half the height of the test section.

Now a_n's indicate the Fourier coefficients when the spanwise distribution of circulation is

expressed in the Fourier series as

$$\Gamma(y)=BU\left(\frac{a_0}{2}+\sum_{n=1}^{\infty}a_n\cos\frac{n\pi}{B}y\right). \quad \cdots\cdots(2)$$

On the other hand, the relation between the swanwise distribution of circulation and lift coefficient is given by the following equation,

$$\Gamma(y)\fallingdotseq\frac{1}{2}UDC_l(y). \quad \cdots\cdots(3)$$

Then the induced angle of attack, α_i, due to the trailing-shed vortex can be calculated by making use of the spanwise distribution of the measured lift coefficient, the truncated forms of Eqs. (1) and (2), and Eq. (3).

(2) The method using θ_m-C_l relation (method (2))

It is thought in general that θ_m may be determined by the width of a wake and the induced velocity. And the width of the wake is thought to vary according to the value of θ_{sb} which is the angular width of the separation region on the cylinder. θ_m decreases as θ_{sb} increases and θ_m increases as α_i increases.

Therefore if the flow around the cylinder is assumed to be two-dimensional potential flow ($\alpha_i=0$), θ_m ought to approach asymptotically the constant value of 90° as θ_{sb} decreases. In the case of three-dimensional flow ($\alpha_i\neq0$), if C_l is large enough, θ_m is scarcely affected by the wake width but by the induced velocity only, because θ_{sb} decreases as C_l increases. This means that θ_m approaches asymptotically the value of $90°+\alpha_i$ as C_l increases. Moreover as mentioned above, since the spanwise distributions of C_l are similar and independent of $C\mu$ in the case of constant λ, it can be shown that α_i is proportional to C_l.

Hence if an asymptote is drawn in Fig. 3 so as to pass the point of $\theta_m=90°$ when $C_l=0$ and approach the experimental values of θ_m as C_l increases, the relation between α_i and C_l ought to be determined from the gradient of this asymptote.

(3) The method using C_l-C_d relation (method (3))

Since the spanwise distribution of $C_l(y)$ is similar, it can be expressed in the Fourier series as

$$\frac{C_l(y)}{C_l}=\frac{A_0}{2}+\sum_{n=1}^{\infty}A_n\cos\frac{n\pi}{B}y, \quad \cdots\cdots(4)$$

where A_n is a function of λ.

A_n in Eq. (4) and a_n in Eq. (1) are related to each other as follows;

$$A_0=\frac{\lambda}{C_l}a_0 \text{ and } A_n=\frac{\lambda}{C_l}a_n. \quad \cdots\cdots(5)$$

Substituting these relations and $y=0$ into Eq. (1) yields α_i at the mid-span, that is,

$$\alpha_i=-\left(\frac{\pi}{4}\sum_{n=1}^{\infty}nA_n\tanh\frac{n\pi}{B}H\right)\frac{C_l}{\lambda}$$

$$=\frac{C_l}{\pi\lambda}\Delta(\lambda), \quad \cdots\cdots(6)$$

where $\Delta(\lambda)$ is a function of λ.

On the other hand, the following relation between the sectional induced drag coefficient, C_{di}, and C_l holds;

$$C_{di} = \frac{C_l^2}{\pi\lambda}\Delta(\lambda). \qquad \cdots\cdots(7)$$

Therefore if the relation between C_l and C_{di} at the mid-span is known, $\Delta(\lambda)$ is determined from eq. (7), then α_i from Eq. (6).

However, it is impossible to know C_{di}-C_l relation empirically, since the profile drag coefficient, C_{do}, is varried according to C_l. Then in this report, two extreme values of C_{do} are assumed for convenience so as to determine the value of C_{di}; they are $C_{do}=0$ and $C_{do}=0.35$.

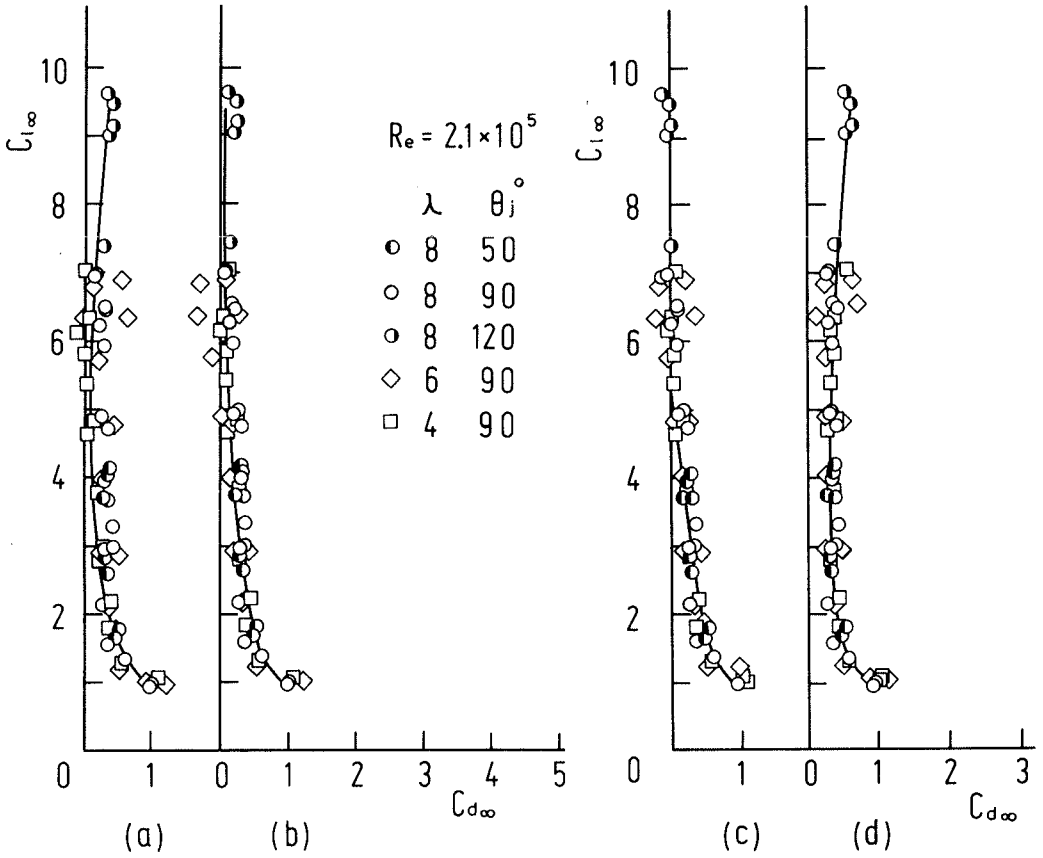

Fig. 6 Relation between $C_{l\infty}$ and $C_{d\infty}$.
(a) metod(1), (b) method(2), (c) case of $C_{do}=0$ in method(3), (d) case of $C_{do}=0.35$ in method(3)

5-2 The corrected experimental values by three different methods

Figs. 6(a), (b), (c) and (d) show the typical examples of the experimental values corrected

by making use of three different methods described in previous section. It seems from these figures that all the corrected experimental values indicate the two-dimensional characteristics of the cylinder fairly well in comparison with the uncorrected values in Fig. 5. And it was concluded by judging from various viewpoints that the most recommended method of them to obtain the two-dimensional characteristics was the case of $C_{do}=0$ in the method (3).

In the case of the method (1), the spanwise distribution of C_l is needed to determine α_i and in spite of laborious calculation, larger scattering is included in the corrected result. Next, although the method (2) is simpler and easier than the others, the degree of error included in α_i is strongly depended on the way how to draw the asymptote in Fig. 3. This means that there is the possibility to include a large error in α_i. Finally, in the case of $C_{do}=0.35$ in the method (3), $C_{d\infty}$ has a tendency to increase again after it reaches the minimum value as $C_{l\infty}$ increases, which should not occur. This method seems to estimate the value of C_{di} too small.

Consequently, it is also concluded that the most recommended method to obtain the two-dimensional characteristic values is the case of $C_{do}=0$ in the method (3).

5-3 Two-dimensional characteristics

In this section we present some examples of the two-dimensional characteristic values obtained by making use of the method (3).

Fig.6(c) shows the $C_{l\infty}$-$C_{d\infty}$ relation. This relation is independent of λ and is approximated by a single curve within experimental scatter. $C_{d\infty}$ decreases monotonically as $C_{l\infty}$ increases, and when $C_{l\infty}>5$, $C_{d\infty}$ becomes nearly equal to zero. This result suggests that the flow around the cylinder can be assumed to be approximately two-dimensional potential flow with circulation around it without a wake of the cylinder, when $C_{l\infty}>5$.

Figs. 7 and 8 show the relation of $\theta_{m\infty}$ and $\theta_{u\infty}$ to $C_{l\infty}$, respectively. Though the uncorrected values of θ_m approach asymptotically the value of θ_m of $90°+\alpha_i$, as C_l increases in Fig. 3, the corrected values approach asymptotically the value of 90° as $C_{l\infty}$ increases. When $C_{l\infty}>5$, $\theta_{m\infty}$ has approximately the value of 90°. This result is corresponding to that obtained from Fig. 6(c).

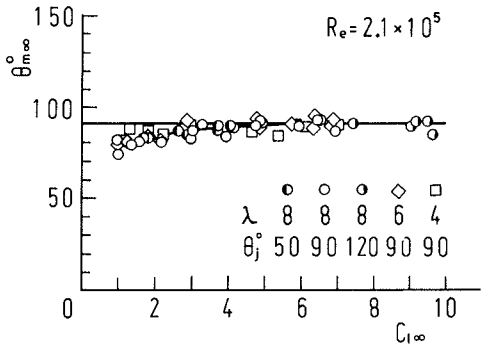

Fig. 7 Relation between $\theta_{m\infty}$ and $C_{l\infty}$.

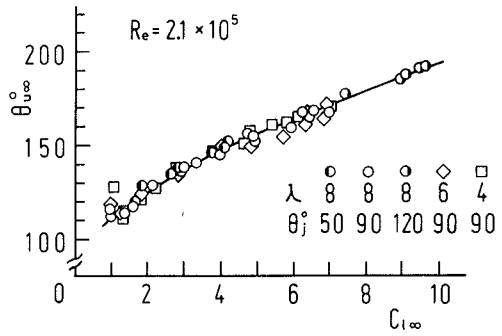

Fig. 8 Relation between $\theta_{u\infty}$ and $C_{l\infty}$.

6 Conclusion

Three different methods of data reduction were devised to obtain the two-dimensional characteristic values of the circular cylinder with tangential blowing. The experimental values were corrected by making use of these methods. The conclusions are as follows;

(1) All the results corrected by three different methods give good two-dimensional approximations of the aerodynamic chracteristics of the cylinder with tangential blowing.

(2) The most recommended method of them is the case of $C_{do}=0$ in the method (3).

(3) It is possible to assume that the flow around the cylinder is two-dimensional potential flow with circulation around it, when $C_{l\infty}>5$.

References

(1) Waka, R., et al., Proc. Int. Symp. Flow Visualization, Bochum, (1980), 528.

(2) Yoshino, F., et al.,Bull.JSME, **24**-192(1981-6), 926.

(3) Yoshino, F., et al., Transactions of JSME, **46**-410(1980-10),1890.

(4) Waka, R., et al., Preprint of JSME, No. 825-1, 76.